Experimental study of the competition between Kondo and RKKY interactions for Mn spins in a model alloy system

J.J. Préjean,[1,] [*] E. Lhotel,[1] A. Sulpice,[1] and F. Hippert[2]

[1] Centre de Recherches sur les Très Basses Températures, CNRS, BP 166
F-38042 Grenoble Cedex-9, France
[2]Laboratoire des Matériaux et du Génie Physique, ENSPG,
BP46, 38402 Saint Martin d'Hères Cedex, France.

The quasicrystal $Al - Pd - Mn$ is a model system for an experimental study of the competition between Ruderman-Kittel-Kasuya-Yoshida (RKKY) and Kondo interactions. First, specific of such alloys, only a few Mn atoms carry an effective spin and their concentration x is tunable over several orders of magnitude, even though the Mn amount is almost constant. Second, the characteristic energy scales for the interactions lie in the Kelvin range. Hence we could study the magnetization on both side of these energy scales, covering a range of temperatures [0.1-100 K] and magnetic fields ($\mu_B H/k_B = 0$ to 5 K) for 22 samples and x varying over 2 decades. Using very general Kondo physics arguments, and thus carrying out the data analysis with no preconceived model, we found a very robust and simple result: The magnetization is a sum of a pure Kondo ($T_K = 3.35K$) and a pure RKKY contributions, whatever the moment concentration is and this surprisingly up to the concentration where the RKKY couplings dominate fully and thus cannot be considered as a perturbation.

I. INTRODUCTION

In the early seventies, experimentalists met the problem of the competition between Kondo and RKKY interactions when studying the magnetic properties of dilute alloys. The latter were noble metals in which one adds $3d$ transition atoms, called "impurities", such as Fe in Cu[1]. Later, this problem arose again when concentrated alloys, containing rare earth elements such as Ce or Yb, became the subject of numerous studies. From a theoretical point of view, to solve this problem remains a challenge in contrast with the two limiting cases (pure RKKY, pure Kondo) which are well understood. It is mainly because the two interactions originate from the same anti-ferromagnetic coupling $\lambda \mathbf{S}.\mathbf{s}$ which develops on the moment site between the spin S of the local moment and the spins s of the conduction electrons. Consequently the same ingredients govern the two characteristic energy scales which emerge in this problem, although in a different way. These ingredients are the exchange constant λ and the electronic density of states (DOS) at the Fermi level, denoted ρ in the following. One energy scale is the *bare* Kondo temperature[2] defined in the absence of RKKY couplings: $T_{K0} \propto E_F \times \exp\left[-1/|\lambda|\rho\right]$. It characterizes a single moment effect: The coupling between the local moment and the surrounding electronic cloud leads to the formation of a non-magnetic singlet when the temperature is decreased below T_{K0}. The other energy scale originates in the RKKY interaction $J_{ij}\mathbf{S_i}\mathbf{S_j}$ which couples the spins of two moments i and j, r_{ij} apart. This interaction is mediated by the spin polarization of the conduction electrons which is induced by the $\lambda \mathbf{S}.\mathbf{s}$ couplings. The $J_{ij} \propto \lambda^2\rho \times cos(2k_F r_{ij})/r_{ij}^3$ alternates in sign rapidly with distance, generating either a ferromagnetic or an anti-ferromagnetic interaction between the two moments, according to the value of r_{ij}. Thus, for given λ and ρ values, the only experimental parameter which can modify the relative weight of the RKKY and Kondo interactions is the distance r_{ij} which governs the pair interaction J_{ij}. In real alloys, one deals with a collection of moments. For this case, one has first to turn to a macroscopic level to define an energy scale T_J characterizing the presence of RKKY couplings. In the same way as we defined T_{K0} in the absence of RKKY coupling, we can define symmetrically T_J in case of a vanishing Kondo interaction for all spins. In real alloys, when Kondo effects are negligible, one can identify the T_J with the temperature at which a magnetic transition occurs due to the RKKY couplings. This transition can be either (anti)ferromagnetic-like for regular systems or spin-glass-like for sufficiently disordered configurations. Let us consider in the latter category systems where the moment concentration x can be varied, whereas the non magnetic matrix remains unchanged. Then, the mean distance $\bar{r}$ between moments is the only variable parameter which allows to change T_J, the T_{K0} remaining constant (at least when λ and ρ are unaffected by the introduction of foreign chemical species in the matrix). In this case, T_J scales with x because $J_{ij} \propto 1/r_{ij}^3$ and $1/\bar{r}^3 \propto x$. In the present paper, we are interested in this type of systems. At this stage, let us consider the optimum conditions necessary to carry out a thorough experimental study. First, the best is to have compounds where T_J, and thus x, can be actually varied *by orders of magnitude*, because of the logarithmic Kondo behavior. The second condition concerns the magnitudes of the characteristic temperatures. Indeed, for each sample, it is desirable to perform measurements at temperatures T (and $\mu_B H/k_B$

for field studies) ranging from well below up to well above T_J and T_{K0}. In practice, it means characteristic temperatures lying in the Kelvin range for magnetization studies because of the temperature and field ranges of the available magnetometers. Note that the most favorable case[3] is that where the magnetic atoms are Mn^{++} with their $g = 2, S = 5/2$ ground state. They exhibit a zero orbital moment, thus an isotropic low temperature Kondo singlet which is not sensitive to crystal field effects.

To satisfy fully all the previously mentioned conditions is difficult to achieve for most dilute alloys because of the solubility limit (Fe in Cu for instance), the magnitude of T_{K0} (> 10 K for Fe in Cu, < 5 mK for Mn in Cu) and/or a large orbital moment. In contrast, the $Al - Pd - Mn$ quasicrystalline (QC) phase satisfies these conditions. Consider two opposite behaviors described previously in separate papers. The first one is that of a $Al - Pd - Mn$ QC sample, here denoted by R, which behaves as a pure spin-glass[4]. See Fig.1: Here, the reported magnetization $M(T)$ is measured in a very small d.c. field $H = 8.6$ Oe. So one can identify the linear susceptibility χ with M/H. The sample was first cooled down to 2 K in zero field. Then the field was applied and M was measured at increasing temperatures. In this so-called zero-field cooling process (ZFC), M is found to exhibit a cusp at a temperature T_g equal to 3.6 K. When the sample is cooled from high temperatures down to 2 K in 8.6 Oe (field-cooling process), the magnetization equals that measured in ZFC down to about T_g but exhibits a plateau below T_g. In addition, one notes that the $\chi(T)$ follows a pure Curie behavior above T_g, from 4.5 K up to 100 K. This is clearly evident in Fig.2 where χ is observed to vary linearly with $1/T$. Altogether the susceptibility cusp, this type of observed magnetic hysteresis and the Curie behavior just above T_g are characteristic of spin glasses. Moreover, the pure $1/T$ dependence of $\chi(T)$ from about T_g up to $30 \times T_g$ indicates an equal weight of the ferromagnetic and anti-ferromagnetic interactions. In summary, no indication of the presence of Kondo effects is apparent in this sample and, in this case, T_J can be identified with T_g: $T_J = 3.6$ K. The opposite case is provided by a sample, here denoted by $B-b$ as in Ref.5, the magnetic behavior of which could be dominated by the Kondo couplings. This sample is less magnetic by two orders of magnitudes than sample R: It can be readily seen from the comparison between the two vertical scales used in Fig.2 to represent the susceptibility of both samples in the same diagram. It follows that, in the absence of Kondo couplings, one should find a T_J for sample $B-b$ about 100 times smaller than that of sample R, thus equal to 30-50 mK. Besides that, we could not detect any susceptibility cusp nor magnetic hysteresis down to 100 mK for this sample, as shown in Sec. III. Another strong difference with the behavior of sample R is the occurrence of a marked continuous curvature of the $\chi(1/T)$ curve over the whole [2 K-150 K] T-range: See Fig.2. One notes that this curvature is negative: When T is decreased, the χ is smaller and smaller than that given by
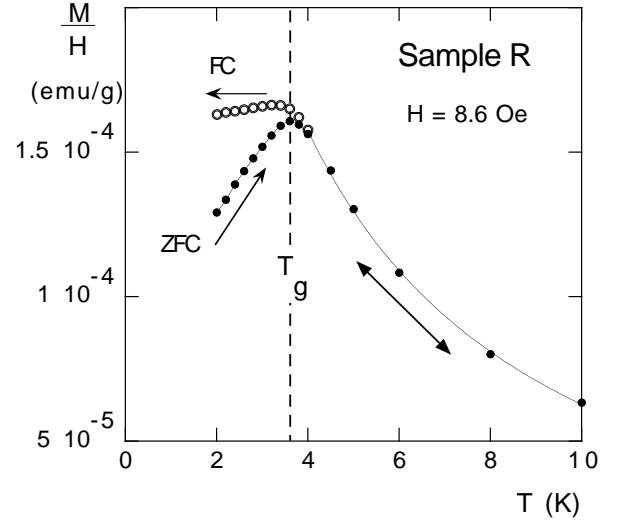

FIG. 1: Magnetization M for $H = 8.6$ Oe of sample R represented in a diagram M/H vs. T for T from 2K up to 10K. The zero-field-cooled (ZFC) magnetization (solid circles) exhibits a cusp at a temperature $T_g = 3.6$ K. Below T_g, the field-cooled (FC) magnetization (open circles) exhibits a plateau characteristic of spin-glasses. The curves are guides for the eye.
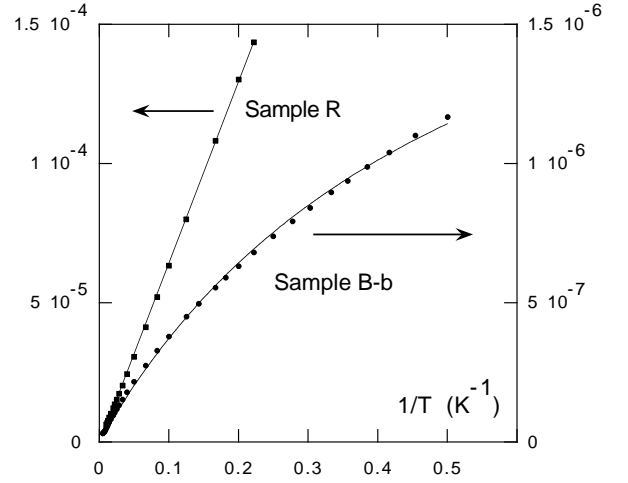

FIG. 2: Susceptibility of samples R and $B - b$ shown in a diagram χ vs. $1/T$. The solid curves are fits: linear fit for sample R and Curie-Weiss fit for sample $B - b$.

$\chi \propto 1/T$ of a noninteracting ($T_{K0} = 0; T_J = 0$) paramagnet. This suggests the presence of antiferromagnetic-like interactions. The problem is to know their origin: Kondo or RKKY couplings? In particular, local chemical order which can exist in dilute alloys is known to lead to large deviations from a Curie behavior[6] at $T \gg T_g$. Actually, in the present case, transport results are in strong favor of the presence of Kondo couplings: See Ref.7 where the present sample is denoted $B - II$. Within the Kondo hypothesis, the order of magnitude of the Kondo temperature T_K can be obtained from a Curie-Weiss fit of

the susceptibility: $\chi = C/(T + \theta)$, over a restricted temperature range. For sample $B - b$, one finds $\theta = 2.5$ K when the analysis is performed from 10 K to 150 K, thus a T_K ($\sim \theta$) lying in the Kelvin range. At this stage, the question is the following: How does the magnetic behavior evolve when one changes progressively the moment concentration from that of sample $B - b$, with presumably dominating Kondo couplings, to that of sample R with pure RKKY couplings ? To answer this question, we performed a study for 22 samples with a x varying by 2 orders of magnitude spanning its range from that of sample $B - b$ to sample R.

Up to now, we have put aside the specificity of the Mn magnetism in the QC phases. But we must consider, even briefly, the very intriguing problem of the formation of effective moments in the present material. First, we recall that the $Al - Pd - Mn$ QC phase is thermodynamically stable only for a narrow range of compositions, containing a rather large amount of Mn, about 8 at%. But only a very few Mn atoms appear to carry an effective spin. Interestingly enough for our study, the fraction of magnetic Mn has been found to vary by orders of magnitude just from very slight composition changes[5]. This is even more interesting in our case since Mn atoms are a component of the structure. Thus those Mn atoms carrying an effective spin are not considered as a different chemical species. So the electronic structure could be very little affected by large variations of the moment concentration, which is a singular advantage that standard alloys cannot present. To give more details, let us recall that the Curie constant of $Al - Pd - Mn$ QC is found to be two or three orders of magnitude smaller than that calculated when all the Mn atoms are assumed to carry a spin $S = 5/2$. For instance, the Curie constant of sample R ($B - b$) is 17 (2000 respectively) times smaller than that expected if all the Mn atoms carry a spin $5/2$. The latter is calculated from the standard formula for the Curie constant of a paramagnet: $C = \alpha x S(S + 1)$, with $\alpha = Ng^2\mu_B^2/3k_B$, $g = 2$ (N denotes the total number of atoms). Note that the only measurement of the Curie constant, $\propto xS(S+1)$, cannot provide separate values of x and S. So, because the x value is *a priori* unknown in any sample, several studies must be carried to deduce the magnitude of S: One could get a S value equal to about $5/2$ from the analysis of the field curvatures of the magnetization[4,8], taking into account the magnetic interactions. Consequently, the x value must be small to explain the magnitude of C, which has been confirmed by NMR studies[9,10] which locally probes the magnetism: Most of the Mn atoms do not carry an effective electronic spin (at least at the time scale of the nuclear relaxation). In the present paper, we are interested in the interactions which affect the few Mn atoms which do carry an effective spin.

The paper is organized as follows. We present briefly our samples in Sec. II and the linear susceptibility data in Sec. III. In Sec. IV, we analyze the $\chi(T)$ with Kondo models (first with a single T_K and subsequently with a broad T_K distribution), which we extend to the magnetization in larger fields. The summary, discussion and possible microscopical pictures are developed in Sec. V before the conclusion (Sec. VI).

II. SAMPLES AND EXPERIMENTAL

Let us recall that the quasicrystals are metallic phases which exhibit a long range order with a five-fold symmetry. In the case of the thermodynamically stable $Al - Pd - Mn$ QC phase, one can grow large sized single grains of high structural quality. It is very favorable for our study because the moment concentration is very sensitive to both the chemical composition and local atomic order[5]. So the best is to avoid grain boundaries where the moment concentration could be different from that in the bulk. We studied 22 samples issued from 15 pieces cut in 11 single grains (denoted by capitals) of slightly different composition (within 21.5-22.5 at% of Pd and 7.5-8.7 at% of Mn). The grains were grown with the Czochralski method. We drew advantage of the sensitivity of the moment concentration to the annealing procedure to get successively "samples" of different moment concentration from the same QC piece, as described in Ref. 5. For samples cut in grains A, B, C, E, G, H, one can refer to a previous paper[5] where many details are given about the preparation, the composition, the required precautions for cutting pieces of homogeneous composition, the heat treatments and the atomic structure. Here the sample notations are those used in Refs.5 and 7. For 18 samples, partial magnetic studies have been previously published[4,5,7], but with no systematic Kondo analysis. The only sample which is not issued from a single grain is that denoted R. It is melt-spun because of its composition, $Al_{71}Pd_{18}Mn_{11}$, out of the stability range. It is more magnetic than the present other samples and thus one expects the presence of grain boundaries to be of little importance, because the average moment concentration is large in this sample. We measured the magnetization and the susceptibility of all samples using SQUID magnetometers described in Ref.5. All the data presented in the following are corrected from the diamagnetic contributions in the way indicated in Ref.5.

III. MAGNETIZATION AND SUSCEPTIBILITY

The main features of the magnetization M of sample $B - b$ are shown in Fig.3 where we represent its field dependence measured up to 50 kOe ($\mu_0 H = 5$ Tesla) at different constant temperatures $T \geq 2K$. The $M(H)$ curves follow the behavior of a magnetization due to localized moments in a paramagnetic regime. Indeed, first, the initial slope, that is the linear susceptibility χ, decreases continuously at increasing temperatures. Second, the magnetization is H-linear up to fields larger and larger at increasing temperatures. It allows one to escape
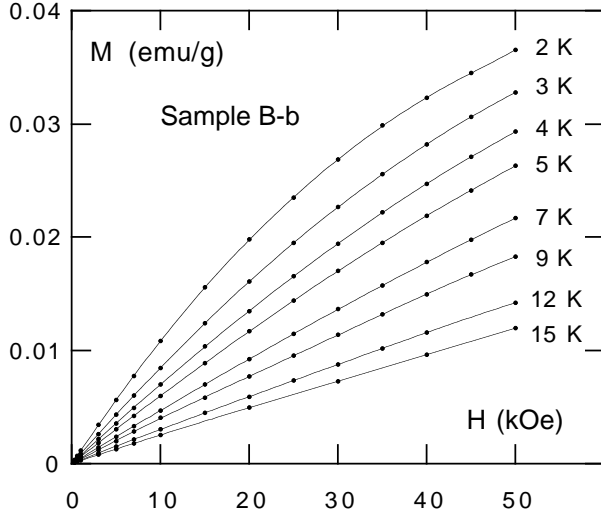
FIG. 3: Field dependence of the magnetization M [corrected from the diamagnetic contribution (in emu/g): $\approx -4 \times 10^{-7} \times H$] for sample $B-b$ at different constant temperatures ($T \geq 2$ K). The curves are guides for the eye.

systematic measurements of $M(H)$ at fixed temperatures to deduce $\chi(T)$. Indeed, it is sufficient to measure the magnetization $M(H_m, T)$ as a function of the temperature in a constant measurement field H_m. The condition to identify $\chi(T)$ for $T \geq 2$ K with $M(H_m, T)/H_m$ is simply that H_m lies in the initial field range where $M(H)$ is field-linear to better than 1% at 2 K. We used this method to obtain the χ data of all the samples shown in Fig.4. For some selected samples, we have also measured the magnetization in d.c. fields and the low frequency (1 Hz) a.c. susceptibility $\chi_{a.c.}$ down to 100 mK. For the very weakly magnetic sample $B-b$, we could not detect any a.c. susceptibility peak down to 110 mK. For more magnetic samples, namely $C-a$, $E-a_2$ and $E-a_3$, the $\chi_{a.c.}(T)$ is observed to exhibit a cusp at a sample dependent temperature denoted T_g: See Fig.5. These data add to those previously published[4] for more magnetic samples: $M-a$ ($T_g = 1.1$ K) and R ($T_g = 3.6$ K). We also studied the zero-field cooled and field cooled magnetizations obtained in d.c. fields below T_g for samples $E-a_2$ and $E-a_3$: We recovered the same magnetic hysteresis features (not shown here) as those observed for sample R presented in Fig.1.

Let us summarize our results. First, we have studied samples which allow us to follow the evolution of the magnetic behavior when changing the moment concentration over two orders of magnitude: From that of $B-b$ to that of sample R. Second, the same sample exhibits continuous $\chi(1/T)$ curvatures at moderate and large temperatures, here attributed to Kondo effects, and a spin glass transition at low temperature, that we showed for several samples. Third, we observe an opposite variation of the relative weights of the Kondo and RKKY effects. On one hand, the T_g is found to increase for samples which
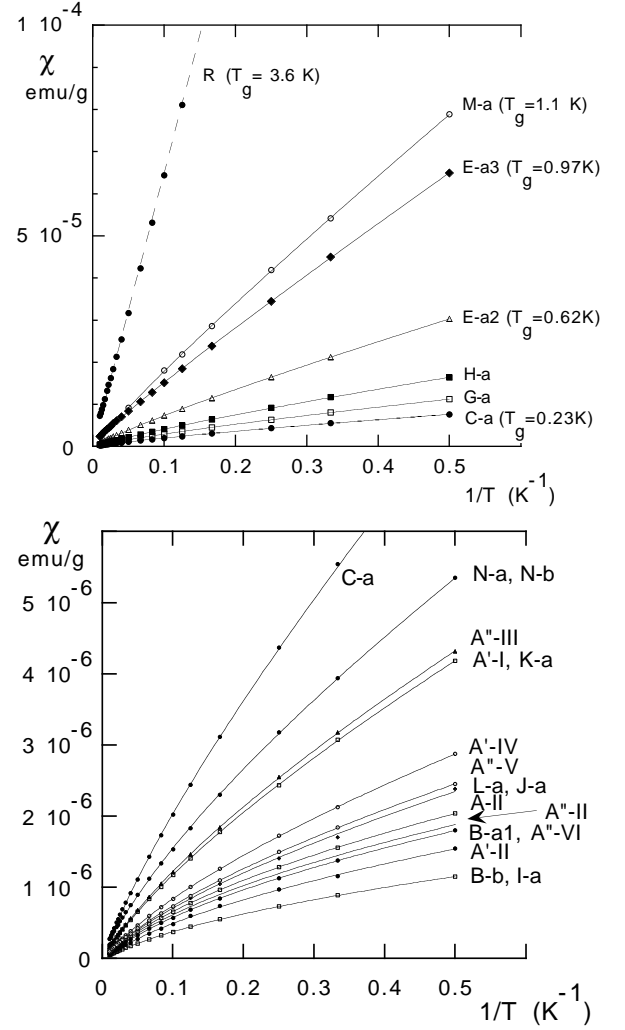

FIG. 4: The d.c. susceptibility (for $T \geq 2K$) is represented in a diagram χ vs. $1/T$ for 22 samples. Here, $\chi = M/H_m$ (see text) with $H_m = 1$ kOe for all samples except for the more magnetic ones: 200 Oe for $E-a_2$ and $E-a_3$ and about 10 Oe for $M-a$ and R. Note the different vertical scales required by the drastic sample-dependence of the susceptibility. The solid curves are Kondo fits within the one-T_K model

are more and more magnetic. Thus with increasing moment concentration: From 0.23 K for sample $C-a$ up to 3.6 K for sample R (See Fig.5 in connection with Fig.4). This feature agrees well with the behavior expected for RKKY spin-glasses. On the other hand, the $\chi(1/T)$ curvatures are found to decrease with increasing moment concentration. This can be observed directly from the evolution shown in Fig. 4 and appears even clearer in Fig.6 where we plotted χ/C^* vs. $1/T$. Here, C^* is a parameter calculated for each sample in order to get the best superposition as possible of the $\chi(1/T)$ curves in the [20K-100K] T-range. Although purely phenomenological, this plot shows that the curvature of $\chi(1/T)$ is more and more pronounced when the sample is less and
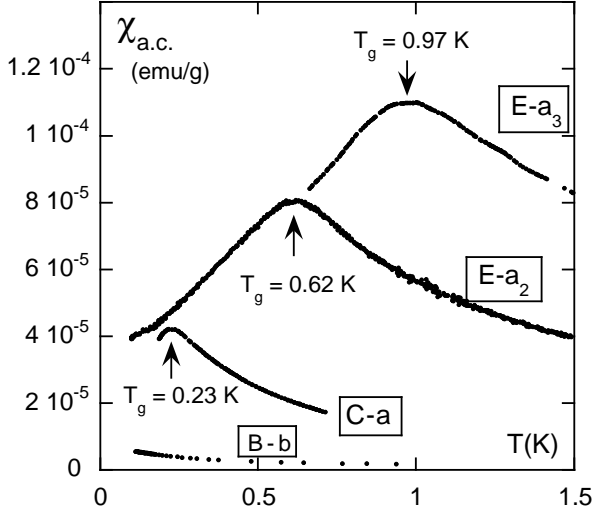
FIG. 5: Temperature dependence of the a.c. susceptibility $\chi_{a.c.}$ for four samples ($h_{a.c.} = 1$ Oe, frequency 1 Hz). Note that T_g values of 1.1 K and 3.6 K have been reported for samples $M - a$ and R in Ref.4
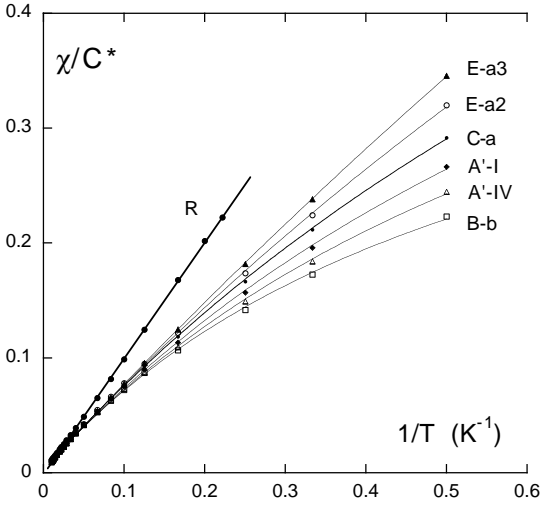

FIG. 6: Normalized susceptibility $\chi/C*$ vs. 1/T. Only a few curves are shown for sake of clarity.

less magnetic. Thus when the single-moment limit is approached: Compare Fig.6 and 4. Surely, this observation reinforces our hypothesis of Kondo effects being at the origin of the $\chi(1/T)$ curvatures. But in turn, this shows that the RKKY couplings end by killing the $\chi(1/T)$ curvatures when the moment concentration is increased. At this stage, one needs a quantitative data analysis in order to understand the relative role of the RKKY and Kondo interactions. This is the aim of the next section.

IV. QUANTITATIVE ANALYSIS

We attributed the $\chi(1/T)$ curvatures observed above 2 K, thus above T_g, to Kondo effects. So, we chose to analyze these curvatures in a very simple way, i.e. fitting our data with a pure Kondo model. Only in a second step, we shall discuss the evolution of the values of the fitting parameters with the moment concentration and, thus, in view of the RKKY coupling effects. In a first attempt (Sec. IV A), we use the simplest Kondo model with a single interaction energy scale (denoted T_{Keff}) for a given sample. Subsequently (IV B), we extend the analysis when assuming the existence of a broad T_K distribution.

A. One-T_K Kondo analysis

We first analyze the $\chi(T)$ data using a genuine Kondo model implying only one energy scale, T_K. Instead of fitting these data with a Curie-Weiss law, we use the results[3,11,12] obtained from the n-channel Kondo model, assumed to be suited to the case $S > 1/2$. In case of $n = 2S$, the Kondo susceptibility $\chi_K(T)$ for $S > 1/2$ behaves as that for $S = 1/2$. In particular, it reaches a saturated value $\chi_K(T = 0)$ ($\propto 1/T_K$) when $T \to 0$, in strong contrast with the Curie susceptibility which diverges as $1/T$. With the definition of T_K given in Appendix A, one obtains Eq.A3 and thus:

$$\chi_K(T, T_K) = \frac{0.616 \times \alpha x S}{T_K} F(\frac{T}{T_K}), \text{with } F(0) = 1 \qquad (1)$$

where $\alpha = Ng^2\mu_B^2/3k_B$ and where we put $S = 5/2$. $F(T/T_K)$ has been found[11,12] to be almost independent on S at low and moderate T/T_K. Thus it can be identified with that one obtained for $S = 1/2$. In the present section, we neglect the deviations (commented in Appendix A) of $F(T/T_K)$ from the $S = 1/2$ results at larger T/T_K. So, we fit the $\chi(T)$ data at all temperatures, using the $F(T, T_K)$ (shown in Fig.7) calculated numerically from the $S = 1/2$ results[13,14] and as explained in Appendix A. The fit is quite satisfactory for each sample over two temperature decades, from 2 K up to 100 K. In Fig.4 the solid curves are the fitting curves. For each sample, the fit provides the values of two parameters: The Kondo temperature which governs the $\chi(1/T)$ curvature and the moment concentration which governs the susceptibility amplitude. The present analysis being a first attempt, we cannot assert however at this stage that the latter parameters represent really the actual Kondo temperature and the exact moment concentration. Thus, in the following, we call them an *effective* Kondo temperature T_{Keff} and an *effective* moment concentration x_{eff} respectively. Once the T_{Keff} and x_{eff} are deduced from the susceptibility of each sample, we can replot the $\chi(T)$ data of all the samples in the scaling diagram: $\chi \times T_{Keff}/(0.616\alpha S x_{eff})$ vs. Log(t) with
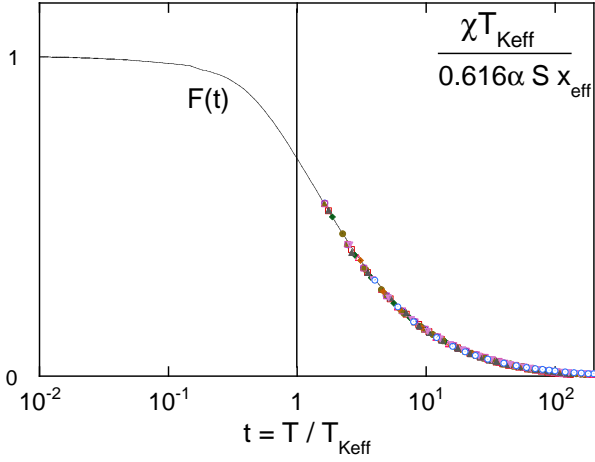
FIG. 7: Kondo scaling for all the samples (except R) for $T \geq 2K$

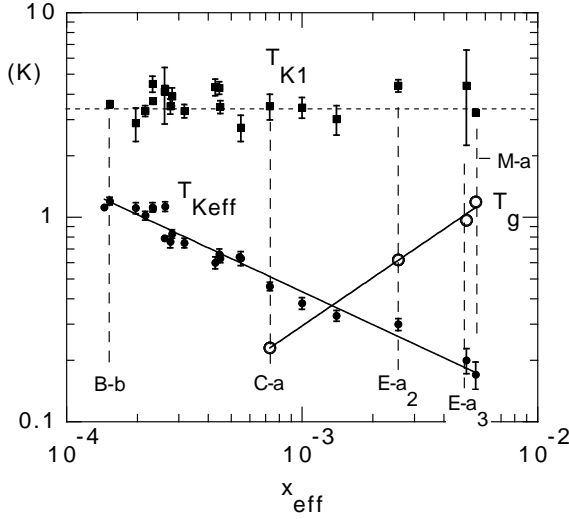FIG. 8: Log-log plot of T_{Keff} (solid circles) and T_{K1} (solid squares) vs. the parameter x_{eff}. The spin-glass temperature T_g (open circles) is reported for four samples. The solid lines are power fits: $T_{Keff} \propto x_{eff}^{-0.55}$, $T_g \propto x_{eff}^{0.8}$.

$t = T/T_{Keff}$, which proceeds from formula Eq.1: See Fig.7. Then, all the data are superposed on the theoretical $F(t)$ curve. Next, we comment on the sample dependence of T_{Keff} and x_{eff}. We found a T_{Keff} varying widely, by a factor 10, when the x_{eff} value varies by a factor 40, from 1.4×10^{-4} for sample $B-b$ to 5.4×10^{-3} for sample $M-a$: See Fig.8. Strikingly enough, the T_{Keff} seems to follow a power law over the present x_{eff}-range: $T_{Keff} \sim x_{eff}^{-0.55 \pm 0.05}$. Qualitatively, the T_{Keff} variation is not really a surprise: The T_{Keff} value reflects the amplitude of the $\chi(1/T)$ curvatures, which was found to decrease at increasing moment concentration. Here, the new result is that we have quantitative T_{Keff} data. In conclusion, it seems possible to fit successfully the $\chi(T)$ data above 2 K with a pure Kondo law. But

one has to investigate the possible origins of the strong dependence of T_{Keff} on x_{eff}. For that, let us assume in the following discussion that x_{eff} reflects the real moment concentration x. Let us first stick to our starting hypothesis of a single energy scale, the T_{Keff}, governing the $\chi(T)$ behavior outside the spin-glass ordered phase. Then, one can imagine two different attractive scenarios, each accounting for the $T_{Keff}(x_{Keff})$ variation. In the first one, T_{Keff} is a standard Kondo temperature but renormalized by the RKKY couplings. This looks reasonable since the value of T_g can be comparable with that of T_{Keff}: See Fig.8. In addition, one observes the T_g to vary with x_{eff} ($T_g \propto x_{eff}^{0.8 \pm 0.1}$) in a way opposite to that of T_{Keff} ($\propto x_{eff}^{-0.55}$). So, one can conjecture T_{Keff} to be a function of both the *bare* (no RKKY) Kondo temperature T_{K0} and the RKKY (no Kondo) energy scale T_J ($\propto x_{eff}$) in such a way that T_{Keff} decreases from T_{K0} at vanishing x_{eff} to zero when x_{eff} increases sufficiently. The second scenario is that of the so-called exhaustion principle[15]. Here, the RKKY couplings above T_g are ignored, but one is interested in the number n_e of conduction electrons available to screen the Mn spins. These electrons are of energy lying within T_K from the Fermi level: $n_e \approx \rho \times T_K$. To treat our case, we use the value of the DOS ρ deduced from specific heat results[4,16,17] and put a T_K equal to 1.2 K which is our largest T_{Keff} value. Then we find a n_e which is, depending on x_{eff}, 70 to 2500 times smaller than the number $2S \times Nx_{eff}$ which should be necessary to screen all the Mn spins. In that case, Nozières[15] proposed to introduce a coherence temperature T_{coh} below which the standard low-T Kondo regime occurs. This T_{coh}, which could be the T_{Keff} in our case, is predicted to equal at most $T_K \times n_e/2SNx_{eff}$, where T_K is the actual Kondo temperature (no exhaustion). It is a prediction ($T_{coh} \propto 1/x_{eff}$) which is qualitatively in agreement with our result: $T_{Keff} \propto x_{eff}^{-0.55}$.

The common feature of the two previous scenarios is a susceptibility reaching its saturation value below T_{Keff}. However, up to now, we only explored the temperature regime above 2 K while we found T_{Keff} values always smaller than 2 K (See Fig.8). So we missed the low-T regime i.e. $T/T_{Keff} < 1$ (See Fig.7) and thus an important data set. However, to extend the Kondo study below T_{Keff} requires a T_g much lower than T_{Keff}. See Fig.8: Sample $B-b$ is a good candidate for such a study. Its T_{Keff} is large (1.2 K) and its T_g, if it exists, is well below 0.1 K (Sec. III). In the diagram χ vs. $1/T$ in the upper part of Fig.9, we show the data obtained down to 2 K together with the Kondo fit which provides the values of x_{eff} and T_{Keff} for this sample. In the lower part of Fig.9 we show the same data plus those obtained down to 110 mK in the same type of diagram but now extended up to $1/T = 10 \ K^{-1}$. Also, we show the previous fit $\chi_K(T, T_{Keff})$ that we extrapolated down to 0.1 K. One could expect the $\chi(T)$ to reach its saturation value below T_{Keff} as suggested from the extrapolated fitting curve. But it is obviously far from being the case: The low-T data are well above this curve. The same feature
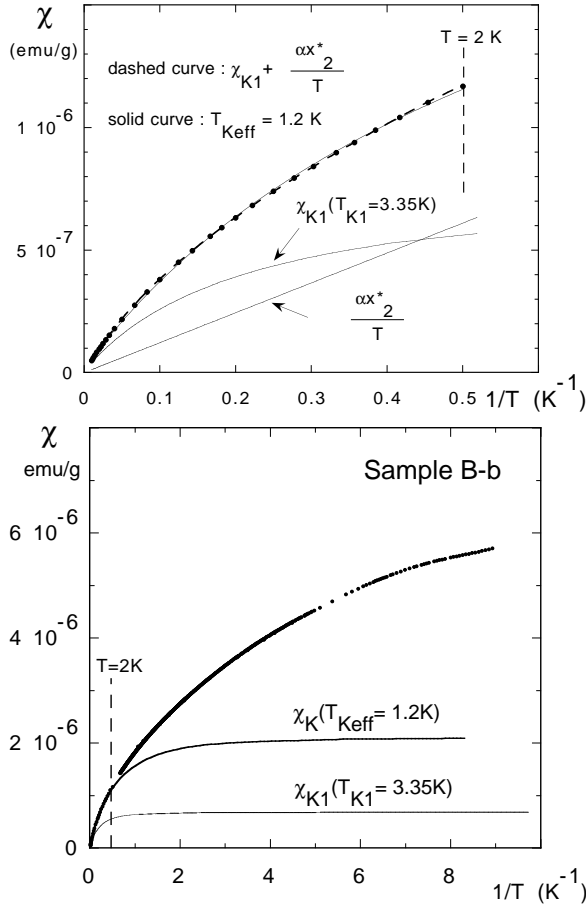
FIG. 9: Susceptibility of sample $B - b$ vs. $1/T$: down to 2 K in the upper diagram and down to 0.1 K in the lower diagram. The susceptibility below 2 K was obtained from d.c. (d.c. field 100 Oe) and a.c. ($h_{ac} = 1$ Oe) measurements. Here we show the Kondo curve fit obtained above 2 K when using a single-T_K (solid curve) and a two-T_K model (dashed curve). Also, we show the $\chi_K(T, T_{Keff})$ fitting curve extrapolated down to 0.1 K, the $\chi_{K1}(T)$ (both diagrams) and $\chi_{K2}(T) = \alpha S x_2 * / T$ (upper diagram) curves calculated with the x_1, x_2^* and T_{K1} values for this sample.

is observed for a more magnetic sample, $C - a$, of smaller T_{Keff} (0.46 K) but nevertheless larger than T_g (0.23 K): See Fig.10. Such results question the validity of our starting hypothesis of a simple ($n = 2S$)-Kondo susceptibility. Two scenarios within the n-channel Kondo model can explain the absence of saturation of $\chi(T)$ when T goes to 0: That one where $n \neq 2S$ with a single T_K and that one where $n = 2S$ but with a broad T_K distribution. For the $n \neq 2S$ scheme, two cases are considered[18]. In the undercompensated case ($n < 2S$), the spin is only partially compensated: It remains a spin $S' = S - n/2$ at low temperature, obeying a Curie behavior ($\chi \propto 1/T$). In the overcompensated case ($n > 2S$), the $\chi(T)$ is expected to vary as $(T/T_K)^{\tau-1}$ at low temperature with $\tau = 4/(n + 2)$. In the case of sample $B - b$, we find a
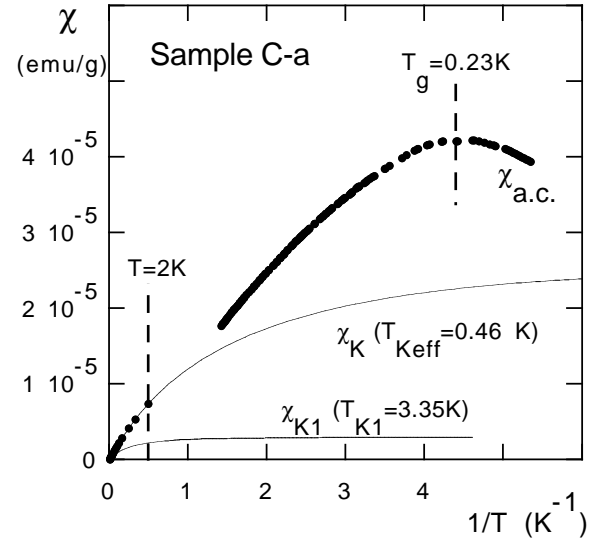

FIG. 10: Same as Fig.9 but for sample $C - a$. The data below 2 K are a.c. susceptibility ($h_{ac} = 1$ Oe).

$\chi(T)$ varying as T^u with u decreasing slightly with the temperature, equal to nearly 0.55 for $0.14 \text{ K} < T < 0.5 \text{ K}$, from which one deduces $n \approx 5$ (hence a spin which has to be assumed smaller than 5/2). However, these ($n \neq 2S$)-models suppose the susceptibility to be governed by a x-independent T_K and thus to be simply proportional to the moment concentration, which is inconsistent with our results. Let us consider the alternative hypothesis: $n = 2S$ but with a broad T_K-distribution $P(T_K)$. Then, the $\chi(1/T)$ curvatures observed well above 2 K could be accounted for by the existence of large Kondo temperatures whereas the absence of saturation of $\chi(T)$ at very low temperatures could be explained by the existence of very low T_K values. In the present case, one has to assume the shape of $P(T_K)$ to depend on the moment concentration to account for our results. Indeed, in this case, the evolution of $P(T_K)$ with the moment concentration leads to that of our fitting parameter T_{Keff} because the latter is obtained from fits carried over a fixed temperature window (2 K-100 K). This working hypothesis is examined in the next section.

B.   Kondo analysis with a T_K distribution

Let us summarize the main result of Appendix B. A Kondo susceptibility $\chi_K(T, T_K)$ averaged over a broad T_K distribution can be described by the sum of a limited number of single-T_K Kondo susceptibilities $\chi_{Ki}(T, T_{Ki})$. For instance, using formula Eq.1 for $\chi_K(T, T_K)$, one can write: $\chi_{Ki}(T, T_{Ki}) = x_i S \times (0.616\alpha/T_{Ki}) \times F(T/T_{Ki})$ where the x_i are parameters having the dimension of a moment concentration. The number of terms in the sum depends on the width of the T-range used for the analysis. If the T-range spreads over two T-decades, one term is

sufficient, implying a Kondo temperature that we identify with our previous T_{Keff}. If the T-range is extended to a third decade, two terms are necessary to describe the susceptibility:

$$\chi(T) = \chi_{K1}(T, T_{K1}) + \chi_{K2}(T, T_{K2}) \quad \text{with} \quad T_{K1} \gg T_{K2} \tag{2}$$

As shown in Appendix B, the value of T_{Keff} lies in between those of T_{K1} and T_{K2}. To fit susceptibility data with the formula Eq.2 is difficult because one deals with $F(T/T_{K1})$ and $F(T/T_{K2})$ which are not simple analytic functions. However, in view of the properties of $F(t)$, we can simplify the analysis in two cases: $T < T_{K1}$ and $T \gg T_{K2}$. Indeed, for $T < T_{K1}$, the χ_{K1} should have reached its saturated value and thus can be replaced by a constant in formula Eq.2. For $T \gg T_{K2}$, the χ_{K2} lies in the high temperature Kondo regime, where the Kondo susceptibility is given by a Curie term with logarithmic corrections. Consequently, one can write: $\chi_{K2} = \alpha x_2 Sq/T$ when the explored temperature range is restricted. The value of the parameter q depends on how the high temperature Kondo susceptibility is parametrized (See Appendix A). In summary, writing $\phi(T, T_K) = \alpha(0.616/T_K)F(T/T_K)$ we propose the following formula:

$$T < T_{K1} : \ \chi(T) = Constant + x_2 S\phi(T, T_{K2}) \tag{3a}$$
$$T \gg T_{K2} : \ \chi(T) \approx x_1 S\phi(T, T_{K1}) + \alpha q x_2 S/T, \tag{3b}$$

Hereafter, qx_2 will be denoted by x_2^*. Let us apply this analysis for sample $B-b$. First, the value of T_{K1} should be larger than 1.2 K, the previous estimate of T_{Keff}. Then, we can fit the data obtained below 1 K ($< T_{K1}$) with formula Eq.3a. The fit provides a value for T_{K2} equal to about 100 mK. Turning now to the analysis of the data obtained at $T \geq 2K$, we note that the T/T_{K2} values are huge in that T-range: From 20 up to 10^3 for T ranging from 2 K to 100 K. It follows that we can apply the formula Eq.3b to fit the data obtained above 2 K. The obtained fit is even better than that carried out with a single T_K (See Fig.9), due to the addition of the third fitting parameter qx_2. The fit provides a value of T_{K1} equal to 3.35 K. Thus, we have explored a T/T_{K1} range, from 0.6 (for $T = 2$ K) to 30 ($T = 100$ K), which allows us to neglect the deviations of $F(T/T_{K1})$ in $\phi(T, T_{K1})$ from the $S = 1/2$ results (See Appendix A). For the other samples ($C-a$, $E-a_2$, $E-a_3$) studied below 2 K, we also observed strong deviations of their susceptibility below 2 K from the extrapolated curve fit $\chi_K(T, T_{Keff})$, as we showed for sample $C-a$ in Fig.10. This stimulates us to reanalyze all the data, even restricted to the [2 K-100 K] T-range, with a two-T_K model and to compare the values of the fitting parameters with those (T_{Keff}, x_{Keff}) deduced previously. It is the subject of the following section.
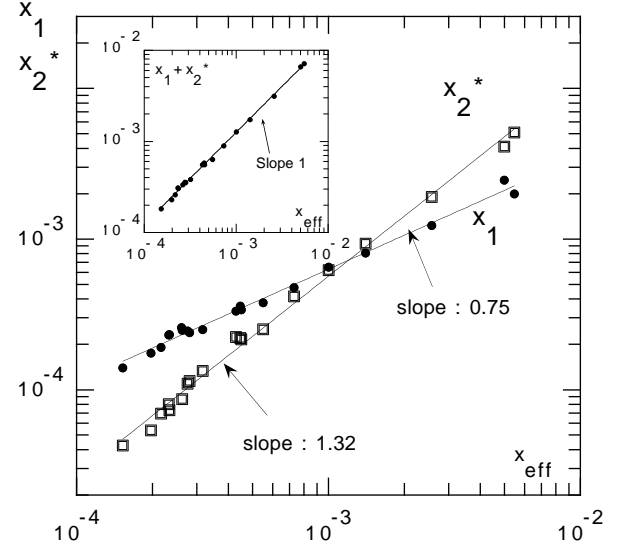

FIG. 11: x_1 and x_2^* vs. x_{eff} and $x_1 + x_2^*$ vs. x_{eff} (inset) in log-log diagrams
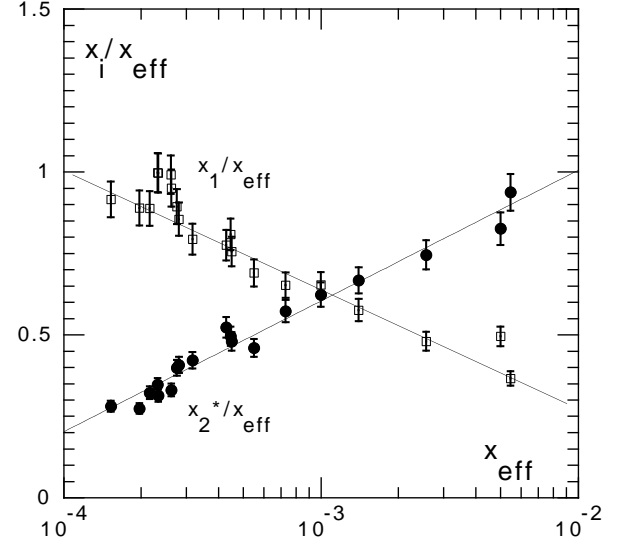

FIG. 12: x_1/x_{eff} and x_2^*/x_{eff} vs. x_{eff} in a semilog diagram. The error bars follow from the relative errors for the determination of x_1, x_2^* and x_{eff}. The lines are guides for the eye

1. Susceptibility

For all samples, the one-T_K Kondo fit of the susceptibility over two T-decades was good. Consequently, an even better fit of the same data using a two-T_K model (formula Eq.3b) is not surprising. Actually, the surprise comes from the remarkable and very simple result provided by the latter fit: The T_{K1} value is found to be constant within our accuracy, i.e. independent on the moment concentration in contrast with the previous T_{Keff} (see Fig.8). More spectacular is that it does so up to
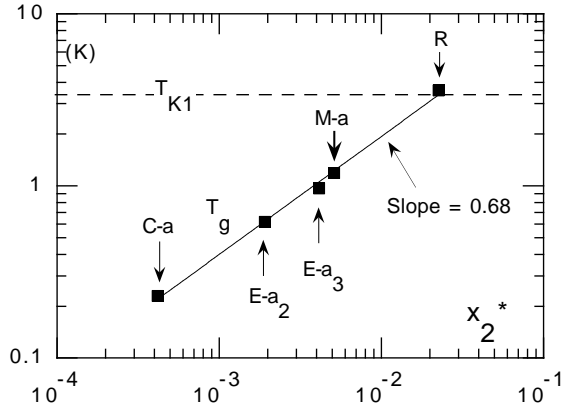
FIG. 13: x_2^* dependence of T_g in a log-log diagram. The x_2^* of sample R is deduced from Eq.3b where we put $x_1 = 0$ since no Kondo $\chi(1/T)$ curvatures can be detected for this sample. The solid line is a power curve fit. The dashed horizontal straight line indicates the value of T_{K1}

the limit where the $\chi(1/T)$ curvatures have almost disappeared (case of sample $M - a$ shown in Fig.4). We propose a value of 3.35 ± 0.15 K for T_{K1}, which is that obtained from data on our largest size samples. Indeed, the accuracy on T_{K1} is mainly determined by that of the susceptibility data which is the better the larger sample mass is (hence the error bars in Fig.8). Another result concerns the amplitude parameters x_1 and x_2^* deduced from Eq.3b assuming $S = 5/2$. First, the sum of x_1 and x_2^* is found to be proportional to the x_{eff} previously deduced: See the diagram in the inset of Fig.11. More precisely, we find $x_1 + x_2^* = 1.32 \times x_{eff}$. Second, both x_1 and x_2^* increase with x_{eff}, but at a different rate: See Fig.11. About the $x_1 + x_2^* \sim x_{eff}$, we find the result obtained in Appendix B from an over-simplified T_K-distribution: A two-T_K analysis provides the same information than the one-T_K analysis about the moment concentration. Let us take x_{eff} as the moment concentration, at least in the following comment of the evolution of x_1 and x_2^* with x_{eff}. Quantitatively, both x_1 and x_2^* are found to follow power laws over the present x_{eff}-range, but with a different exponent value: $x_1 \propto x_{eff}^{0.75}$ and $x_2^* \propto x_{eff}^{1.3}$ as shown in Fig.11. Then, we can deduce the evolution of the normalized distribution $P(T_K)$ with the moment concentration x_{eff}: The weight of the susceptibility term associated to T_{K1} is given by x_1/x_{eff}, while that, x_2/x_{eff}, associated to T_{K2} is reflected by the x_2^*/x_{eff} value. These weights are represented as functions of x_{eff} in Fig.12.

At this stage, we can draw some interesting and simple conclusions. First, we could split the susceptibility into two contributions, each exhibiting a specific behavior. One (χ_{K1}) is Kondo-like with a Kondo temperature (T_{K1}) independent on the moment concentration. The other contribution (χ_{K2}), to which we attribute an almost vanishing Kondo temperature, follows nearly a Curie law above 2 K. The more striking result is that

the behavior of the two contributions holds with the same characteristics when the moment concentration is increased up to that one where the Kondo contribution disappears (sample R). Let us focus now on the (almost) non Kondo contribution to the susceptibility. As shown below, it behaves as the susceptibility of a RKKY spin-glass containing a spin concentration proportional to x_2^*. First, $\chi_{K2}(T) \propto x_2^*/T$ above 2 K. Second, one finds T_g obeying a power law of x_2^*: $T_g \propto (x_2^*)^{0.68}$ and, strikingly enough, it does so over almost two decades of x_2^* when the data for sample R are included: See Fig.13. It is because of this very large x_2^* range that we can deduce the exponent value rather accurately (0.68 ± 0.02) taking into account the relative precision on the (T_g, x_2^*) values. A similar power law governs the T_g dependence on the moment concentration in purely RKKY spin-glasses. Moreover the exponent value equals that found for the canonical $Cu - Mn$ spin-glass[4]. To complete the panorama of the susceptibility features, let us focus on the disappearance of the $\chi(1/T)$ curvatures. It occurs for sample R while $\chi(1/T)$ curvatures are still present for sample $M - a$ which is only 3 times less magnetic (See Fig.4). Thus sample R can be taken as a crossover sample: Its moment concentration could be the minimum one necessary to observe RKKY couplings dominating fully. Another interesting feature is that the T_g becomes comparable with T_{K1} when the concentration is increased up to that of sample R: See Fig.13. We shall discuss these two points in Sec. V. In summary, our analysis gives simple results in the zero-field limit (susceptibility analysis). The question is to know wether such an analysis holds when moderate or even large fields are applied. This is the object of the next section.

2. Magnetization $M(H)$ at 2K

In a general way, one can write the magnetization as: $M = Nx \times g\mu_B S \times P(H, T, T_J, T_K \ldots)$. Here, x and P are the actual moment concentration and average spin polarization respectively. P varies from 0 to 1 when the field is increased from 0 up to values large enough to overcome the temperature and interaction effects. Here, the largest characteristic temperature is T_{K1}. Then, because the maximum field attainable in our magnetometers equals 70 kOe, the available maximum value of $\mu_B H/k_B T_{K1}$ equals 1.4. Surely, this value is not large enough for a complete study of the magnetization up to its saturation value but it is expected to be sufficiently large for generating marked $M(H)$ curvatures suitable for a meaningful analysis. Formally, it is possible to decompose the magnetization of any sample at a given field and temperature as the sum of two terms:

$$M(H, T) = Ng\mu_B S[x_1 P_1(H, T, T_1^*) + x_2 P_2(H, T, T_2^*)] \quad (4)$$

where x_1 and x_2 have the values deduced from the susceptibility analysis. Here, we consider the more general
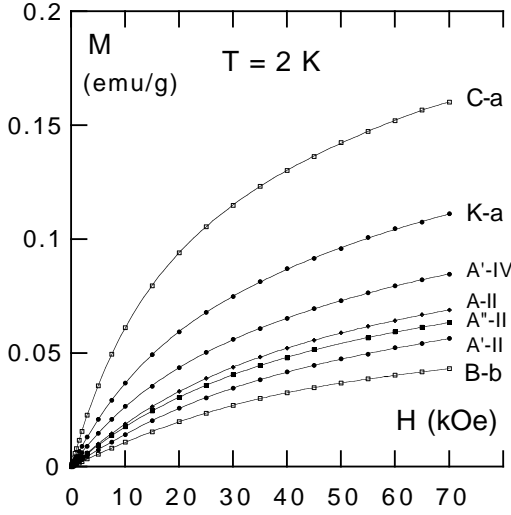
FIG. 14: Magnetization at 2 K of some of the less magnetic samples.

FIG. 15: Scaled magnetization $Y = M/(Ng\mu_B \times x_1 S)$ at constant magnetic field vs. X=x_2^*/x_1. Figures are values (in kOe) of the applied magnetic field. The data $X = 0.9$ are obtained for the more magnetic $(C - a)$ of the samples analyzed here. Error bars, represented only for several constant field values, come from relative errors, 3% at maximum, for the x_1 and x_2^* deduced from the $\chi(T)$ analysis

formula for the $M(H,T)$ decomposition above T_g. We only assume the T_i^* to be characteristic energy scales for the interactions in the presence of a field and we attribute no explicit physical meaning to the P_i. In the zero field limit where $M = \chi H$, formula Eq.4 is equivalent to Eq.2 with $T_1^* = T_{K1}$ and $T_2^* = T_{K2}$. But we have no particular reason to assume that the same simple result holds in large fields, especially when $\mu_B H/k_B$ becomes comparable to T_{K1}. Surely, one can use formula Eq.4 to fit the magnetization data for large fields but, then, each T_i^* could depend on the variable parameters, i.e. H, T and the moment concentration. To clarify this point, we present an analysis of the magnetization measured at 2 K. This temperature has the advantage to lie in-between T_g and T_{K1}. Indeed this allows us to examine $P_1(H)$ in the more relevant, i.e. low-temperature, Kondo regime ($2 K \approx 0.6 \times T_{K1}$) but also to escape the spin-glass order regime ($2 K > T_g$). However spin-glass transition effects do affect the magnetization in moderate and large fields, even well above T_g (See for instance Ref. 8). It is because the terms non-linear in the field of the magnetization increase rapidly (up to exhibit a divergence) when T is decreased down to T_g. Thus, to avoid this additional difficulty, we restricted the magnetization analysis to the samples of T_g smaller than about one tenth of the measurement temperature 2 K. This implies to restrict the study to our less magnetic samples, the more magnetic one among them being $C - a$ of $T_g = 230$ mK. The $M(H)$ data of some of these samples are shown in Fig.14. To analyze our data, we intend to use formula Eq.4. But, in this formula, the parameter x_2 appears explicitly whereas we only deduced previously the value of $x_2^* (= q \times x_2)$ for each sample. As the q value is unknown, we transform Eq.4 as follows:
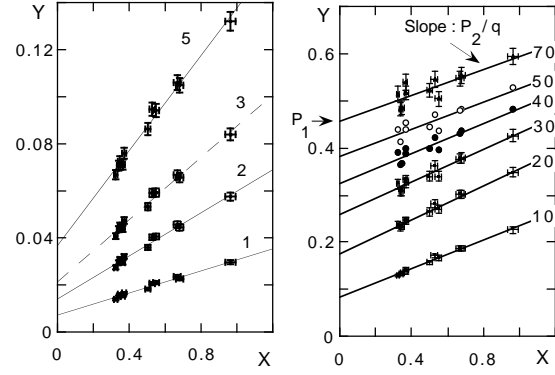
$$\frac{M(H,T)}{Ng\mu_B x_1 S} = P_1(H,T,T_1^*) + \frac{x_2^*}{x_1}\frac{P_2(H,T,T_2^*)}{q}, \quad (5)$$

The formula Eq.5 is interesting because it contains only two unknown parameters: P_1 and P_2/q. Indeed, the sample dependent parameter x_2^*/x_1, denoted X in the following, can be calculated for each sample from our susceptibility results. It increases with the moment concentration since $x_2^*/x_1 \propto x_{eff}^{0.55}$ following the results in Sec. IV B 1. The parameter $M(H,T)/Ng\mu_B x_1 S$, that we denote Y, can be deduced from the measured $M(H,T)$ and the x_1 value. The value of T has been fixed: $T = 2$ K. Let us fix the value of H and analyze Y as a function of X. One finds Y to vary linearly with X, whatever the fixed field value: See Fig.15. This proves that the magnetization obeys Eq.5 with T_1^* and T_2^* independent of the moment concentration. Therefore, we proved that the simple decomposition of the magnetization in terms of two (and only two) independent contributions holds up to large fields. The next step is to examine the field dependence of P_1 and P_2/q at 2 K. At each field value, the values of P_1 and P_2/q are given by the best linear fit of the $Y(X)$ data. We represent them as a function of the field in Fig.16. In this Figure, one observes readily that $P_1(H)$ and $P_2(H)$ behave in a completely different way. P_1 increases continuously with the field, with no tendency to reach its saturated value, even at 70 kOe. This feature is thus in strong contrast with the magnetization of non-interacting spins 5/2, which reaches almost its saturation value above 10 kOe at 2 K. It suggests that P_1 is governed by a large characteristic temperature over the whole field-range. Even more striking, the evolution of $P_1(H)$ with H at 2 K (i.e. $\approx 0.6 \times T_{K1}$) appears to be similar to that of the theoretical Kondo polarization $P_{th}(H/T_K)$ calculated at $T = 0$ for spins 1/2. In Fig.16,
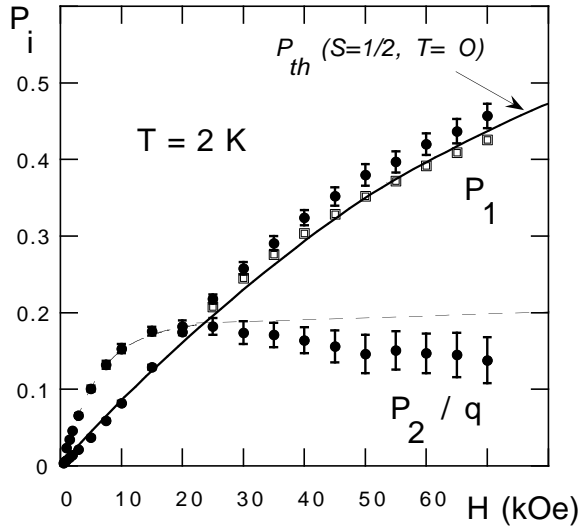
FIG. 16: Field dependence of P_1 and P_2/q (full circles) deduced from the $Y(X)$ linear fits of Fig.15. The error bars originate in the scattering of the Y and X data. The open squares represent the $P_1(H)$ calculated when a constant value (≈ 0.2) of P_2/q is imposed in the $Y(X)$ fit at $H > 25$ kOe. The dashed curve represent the fit of P_2/q by a Brillouin function up to 25 kOe and its extrapolation up to 70 kOe. The full curve represents the theoretical variation of the Kondo polarization for spins 1/2 at 0 K (See text).

the full curve is that of Figure 6.2 in Ref.2 rescaled with our T_{K1} value (3.35 K)[19]. This quantitative similarity calls for three comments. First, it suggests strongly that P_1 is governed by only one energy scale: T_{K1}, over the whole studied field-range. Thus $T_1^* = T_{K1}$ in formula Eq.4 for fields from 0 up to at least 70 kOe ($\mu_B H/k_B T_{K1}$ from 0 to 1.4). Second, because the saturated value of $P_{th}(H/T_K)$ equals 1 in the calculation, that of $P_1(H)$ should do the same, which was not among the starting hypothesis. The third comment is about the fact that the P_{th} has been calculated for spins 1/2 whereas the Mn spins are expected to equal 5/2. In Appendix A, we recall the result obtained for the susceptibility in the ($n = 2S$)-model: A Kondo moment behaves as n Kondo spins 1/2 in view of formula Eq.A3. One of the best possibilities for checking the latter prediction consists in studying the field-curvatures of the spin polarization. Presently, the close agreement between $P_1(H, 2K)$ and $P_{th}(H, T = 0)$ suggests strongly that this prediction is correct and indeed valid up to fields at which the polarization is rather large: See Fig.16. However, some details of the P_1 behavior remain obscure. Up to 3 kOe, P_1 is found to vary linearly with an initial slope identical with the previous χ_{K1} results at 2 K. Note that at this temperature, χ_{K1} equals about 80% of its value at $T = 0$, hence $P_1(H, T = 2K) = 0.8 \times P_{th}(H, T = 0)$ at low fields. But at larger fields, up to 20 kOe, P_1 varies slightly more rapidly than the field, which makes the agreement between $P_1(H, T = 2K)$ and $P_{th}(H, T = 0)$ closer than it could be expected. This feature cannot be explained

by the scattering of the Y and X data and is not predicted theoretically, at least not for spins 1/2. Let us now comment on the P_2/q behavior. It appears to reach a saturation value very rapidly when compared to the P_1 case, which tends to prove that the characteristic temperature for the interactions is very low compared to 2 K. It was the result obtained previously in the zero field limit. Thus we propose: $T_2^* \approx 0$ in formula Eq.4 whatever the field value. Note that the decrease of P_2/q at increasing fields above 30 kOe could be nothing else that an artifact due to the errors in the determination of P_1 and P_2. Indeed, the relative weight of the P_2/q contribution with respect to P_1 decreases at increasing fields. This is obvious in Fig.15. In turns, to impose a constant P_2/q value equal to 0.2 in the linear fit of $Y(X)$ above 25 kOe does not change drastically the P_1 values obtained previously: See the open squares in Fig.16. In summary, we have found that the split of the low field magnetization (susceptibility case) into two contributions, each governed by a different energy scale (the T_{K1} and an almost vanishing T_{K2}), holds up to rather large fields over the whole studied field range. We found the P_1 to be described by the theoretical polarization calculated for spins 1/2. Note that we found a saturated value of P_2/q nearly equal to 0.2, Then, if one assumes the saturated value of P_2 to be equal to 1, one deduces a q value equal to about 5. This point is discussed in the next section.

V. SUMMARY AND DISCUSSION

Preliminarily, we have recalled the two opposite limiting cases, pure RKKY and pure Kondo, associated with two distinct energy scales: The T_J ($\propto x$) which characterizes pure (no Kondo) RKKY coupling effects and the T_{K0} which characterizes the single impurity Kondo interaction. Our more magnetic sample (R sample) seems to fall in the first limiting case, that of a x sufficiently large so that only RKKY features are detected. When decreasing the moment concentration, we observed Kondo susceptibility features at moderate and large temperatures and a spin glass transition at lower temperature. This led us to analyze the susceptibility above T_g with pure Kondo models, ignoring temporarily the RKKY interactions. The only additional hypothesis, that of a broad $P(T_K)$, was introduced because we found no saturation of the susceptibility at very low temperature. We found a way for fitting easily our data: It consists in replacing the broad T_K-distribution by a bimodal one. Indeed, both give the same averaged Kondo susceptibility in our T-range, as we showed from a very simple calculation. Of course, because of the bimodal distribution treatment, the susceptibility takes simply the form of a sum of two contributions. A priori, there is no physical meaning in this decomposition which can be achieved for any given sample. It is only by studying the characteristic features of each contribution when varying the moment concentration by two decades that we hit on

a remarkable result: The behaviors of the two limiting cases (pure Kondo, pure RKKY) appear to coexist in the same sample whatever x and are sufficient to describe the $\chi(T)$ and the $M(H)$. In particular, this decomposition holds up to the moment concentration where the Kondo susceptibility features disappear completely. Let us summarize. One contribution appears to obey the characteristic x-independent features of single Kondo impurities in as much as the temperature dependence of the susceptibility (the χ_{K1}) is concerned as well as the low-T field dependence of the polarization (the P_1). Consequently, we conclude that T_{K1} is the bare Kondo temperature T_{K0}. The other contribution is that one expected for a pure RKKY spin-glass: The T_K is (almost) vanishing, the susceptibility (the χ_{K2}) varies as $1/T$ above T_g, the T_g varies with x_2^* as the T_g of standard spin-glasses does with the moment concentration and, finally, well above T_g, the spin polarization (the P_2) reaches its saturated value in a moderate field (at least at 2 K). At varying moment concentration, the characteristics of the two contributions remain unchanged, only their relative weights vary, obeying $x_2^* \propto x_1^{1.8}$ within our concentration range (Sec. IV B). When assuming that x_{eff} does reflect the (a priori unknown) moment concentration, we found that the purely Kondo contribution ($\propto x_1/x_{eff}$) decreases while the RKKY contribution ($\propto x_2^*/x_{eff}$) increases when increasing the moment concentration. Note that even for samples where the Kondo couplings are dominating, thus of very small x_2^*/x_{eff}, the χ_{K2} contribution ends to be spectacularly dominant at low T. Indeed, when decreasing the temperature, the χ_{K1} tends to reach its saturated value whereas the χ_{K2} contribution continues to increase. An example is given for sample $B-b$ in Fig.9: See the $\chi_{K1}(T)$ and $\chi_{K2}(T)$ evolution with temperature. Of course this χ_{K2} dominance at low T is more and more evident when the moment concentration, and thus the x_2^* weight, increases: Compare Fig.10 with lower part of Fig.9. This trend is apparent even above 2 K as it can be seen in Fig.6. Note that finding T_{K1} (identified to T_{K0}) constant whereas the moment concentration x is varied by orders of magnitude proves that the electronic structure is not affected by large x changes. In that sense, our system exhibits the same remarkable property as the heavy fermion $Ce_{1-x}La_xPb_3$ where, fortuitously, T_K and the crystal field splitting are concentration independent, which enabled a proof of single moment properties[20]. In $Al-Pd-Mn$ QC, this property can be attributed to the fact that the moment concentration remains small ($< 1\%$). More fundamentally, it was expected because large variations of the moment concentration can be achieved with minimal changes of the overall number of Mn atoms.

Our results are the more striking as they were obtained from an analysis using only very general hypothesis from the outset. At this stage, let us attempt to explain our results with different models. First, the problem can be treated on a macroscopic scale. For instance, one can assume that the thermodynamic quantities, $\chi(T)$, $M(H,T)$ or the magnetic specific heat $C_P(T)$, can be developed as a series of terms reflecting successively a single-impurity effect (pure Kondo), a two-impurity effect (RKKY)... in the way described in Ref.21. But other hypothesis exist in terms of microscopical models able to yield T_K distributions. In such models, broadly distributed environments of the spins are required to generate a $P(T_K)$. Let us consider several models. The first one is based on strong fluctuations of the local DOS ρ_{local} assumed to trigger the T_K value[22] (as well as the RKKY couplings[23]) instead of the average DOS. To apply this model in case of QC is conceivable due to the multiplicity of local *atomic* environments and specific electronic structure[7]. However this model can hardly provide an evolution of the ρ_{local} distribution with the moment concentration able to account accurately for the evolution of the x_i. Let us now consider microscopical models based on magnetic proximity effects assumed to decrease locally T_K with respect to T_{K0}. Then the T_K distribution is due to the multiplicity of local *magnetic* environments (distances between spins, local spin concentration). This model implies a x-dependent $P(T_K)$. The upper limit of $P(T_K)$ equals T_{K0}. The broadness of $P(T_K)$ is achieved for a lower limit of $P(T_K)$ (almost) vanishing when compared to T_{K0}. In the general case, such a x-dependent $P(T_K)$, even with the upper bounding limit T_{K0}, cannot be expected to give a x-independent T_{K1} when interpreted in terms of a bimodal distribution.

However, it is the latter model that we develop in the following because it can be easily transformed into an *ad hoc* model able to account for our results. Indeed, one can introduce the following two additional assumptions which forces the T_K-distribution to be really bimodal. The first one is a single-impurity Kondo behavior, with $T_K = T_{K0}$, robust enough to apply as soon as the spins are separated by a distance larger than a characteristic length R_C. The second (and perhaps stronger) hypothesis is a T_K collapsing very rapidly as soon as the distance between spins becomes smaller than R_C. In summary, a spin $\mathbf{S_i}$ can be considered as magnetically 'isolated' with a T_K equal to T_{K0} if no other spin lies in a sphere of radius R_C centered at site i. In the opposite case, spin $\mathbf{S_i}$ is 'non isolated' and its T_K is assumed to be (almost) vanishing. In our case, the T_{K1} could characterize the behavior of 'isolated' spins and thus could be identified with T_{K0}. Let us focus on R_C. It may refer to the length scale introduced in different scenario for the T_K-collapse due to proximity effects: See the discussion in Ref.21. The first one is about Kondo cloud overlap: The conduction electrons involved in the different Kondo clouds of radius ξ_K are assumed to be almost orthogonal. So, the single-impurity Kondo model should hold even when ξ_K is larger than the distance between moments. Its breakdown has been predicted only for distances between moments much shorter than ξ_K, at least at 3D[21]. This leads to a R_C which thus is not too large although the formula for ξ_K ($\xi_K = \hbar v_F/k_B T_K$) yields a huge ξ_K value, lying in the μm range for $T_K \sim 1$K

and if one identifies v_F with the standard Fermi velocity of pure simple metals. However, the latter assumption is controversial, the ξ_K could be much smaller. Moreover in QC, the Fermi velocity as defined for free electrons is not pertinent because of the specific electronic properties of QC (flat bands)[24]. Another possible mechanism for the local T_K depression is a RKKY coupling directly competing with the Kondo interaction. Then, one has to compare T_{K0} with a *local* energy scale $T_{J.loc}(i)$ which reflects the RKKY interactions that spin $\mathbf{S_i}$ undergoes from the other spins. One can write: $T_{J.loc}(i) = |\mathbf{S_i} \sum_j J_{ij} \mathbf{S_j}|$ from which a local length scale R_i can be defined: $1/R_i^3 \propto |\sum_j (\mathbf{S_i S_j}/S^2) \times cos(2kr_{ij})/r_{ij}^3|$ so that $T_{J.loc}(i) \propto S^2/R_i^3$. Then a R_C can be naturally defined as the length for which $T_{J.loc}(R_C) \sim T_{K0}$. Consider the two following limiting cases when the temperature decreases. First, if $T_{K0} \gg T_{J.loc}(i)$ ($R_i \gg R_C$), the individual moments are Kondo quenched before the RKKY coupling can become effective. Then the T_K of spin $\mathbf{S_i}$ equals T_{K0}. Second, for $T_{J.loc}(i) \gg T_{K0}$ ($R_i \ll R_C$), the RKKY coupling is fully effective well above T_{K0}, impeding the $\mathbf{S_i}$ to be quenched at lower temperature[25]. In the latter case, when only two spins are involved ($T_{J.loc}(i) = |J_{ij}\mathbf{S_i S_j}|$), the spins of the two impurities compensate each other for an antiferromagnetic RKKY coupling. But if the RKKY coupling is ferromagnetic, one gets a resulting spin $2S$ of behavior different from that of single spins[25]. The problem of comparable $T_{J.loc}(i)$ and T_{K0} is difficult to solve even in the two-impurity case: See Refs 25 and 26 and references therein.

In short, we can use a microscopic model where x_1 and x_2 are actual concentrations of spins, the 'isolated' ones with $T_{K1} = T_{K0}$ and the 'non isolated' ones with $T_K \approx 0$ respectively. Then the actual total moment concentration x equals $x_1 + x_2$. Here we note that the exhaustion problem is not solved when considering only the 'isolated' spins, although $x_1 < x_{eff}$ and T_{K1} is larger than the T_{Keff} considered in Sec. IV A. A calculation similar to that done in Sec. IV A shows that the number n_e of conduction electrons available for the Kondo screening is, depending on x_1, 20 to 300 times smaller than that, $2SNx_1$, necessary to screen all the 'isolated' Mn spins. In addition T_{K1} does not follow qualitatively the $1/x_1$ law predicted to reconcile the exhaustion problem with the possibility to observe a Kondo effect (Sec. IV A). In strong contrast, T_{K1} is constant over our whole concentration range. This calls for further theoretical explanations[27]. Granted that, the present microscopic model well accounts qualitatively for our main results, independently of the T_K-collapse mechanism. Let us start from extremely low moment concentration: The probability x_1/x to have 'isolated' spins should be maximum, thus equal to 1. But it is expected to decrease with increasing moment concentration while that (x_2/x) of the 'non isolated' spins increases, which agrees with the results shown in Fig.12 when x_{eff} is identified with x. Interestingly enough in this model, when the moment concentration is increased up to the limit where the mean

distance $\bar{r}$ between moments equals about R_C, only a few spins are still 'isolated'. Then the system should be (almost) fully dominated by the RKKY interactions and the $\chi(1/T)$ curvatures should have vanished. This is precisely what we observed when the moment concentration x is increased up to that of sample R. Hence we identify the value of R_C with that of $\bar{r}$ ($= a \times x^{1/3}$) of sample R. Here, a is the inter-atomic distance. If x of sample R is simply deduced from the measured Curie constant (assuming $S = 5/2$), one finds a $\bar{r}$ and thus a R_C equal to about $5.3 \times a$ ($13 \mathring{A}$). This model also predicts spin-glass transition features which well agree with our results. Indeed, the 'non isolated' spins can be assumed to undergo RKKY interactions since their T_K is vanishing whatever the T_K-collapse origin is. In addition, because T_g is smaller than the T_{K1} of the 'isolated' spins, the latter should be Kondo quenched and thus transparent for the RKKY interactions at T_g. Hence, for the spin-glass transition, the sample behaves as if the only existing spins are the 'non isolated' ones. It follows a T_g expected to obey a power of x_2 with a standard exponent value (≈ 0.7), which we precisely found experimentally.

More surprisingly, in view of the crudeness of the underlying hypothesis, the predictions of the present model account even quantitatively, and not only qualitatively, for our results, as shown below. This is the more correct, the smaller the moment concentration in order to have only 'isolated' spins and pairs, but not triplets, of spins with $r_{ij} < R_C$. Then, the pair concentration is small, so each pair, which occupies a small region (linear size R_C) in the space, is separated from the other ones by large distances. Consequently, the RKKY interaction should be rather strong between two spins of a pair (because $J_{ij} \propto 1/r_{ij}^3$ and $r_{ij} < R_C$), but much smaller between the spins of two different pairs because of the distance ($\gg R_C$) between pairs. Then one expects the RKKY coupling to generate distinct effects depending on the temperature range. When the temperature is decreased, the first effective RKKY interactions are those coupling two spins in a pair, forming a ferromagnetic F-pair (spin $2S$) or an antiferromagnetic AF-pair (spin 0) depending on the value of $k_F r_{ij}$. It is only at much lower temperature that the spins $2S$ of the F-pair undergo RKKY couplings from the other ones to yield a spin-glass transition. This picture implies that P_2, which becomes a polarization of true moments in the model, is a polarization of F-pairs at moderate T. This agrees with our P_2/q results for the less magnetic samples (Sec. IV B 2): We found P_2/q at 2 K to scale with a Brillouin law (See Fig.16) with a spin value equal to nearly 4, thus comparable with the resulting spin of a F-pair of two spins $S = 2$. However, two additional conditions have to be introduced to achieve a quantitative agreement. The first one is an equal probability to have F and AF pairs, which is expected for perfect disordered configurations because of the very rapid oscillations of the RKKY coupling with distance within R_C. The second condition is a large S value. This allows to account for χ_{K2} vary-

ing simply with $1/T$ over the whole T-range above T_g because the Curie constant for a collection of such pairs can be considered as temperature independent. As an example, consider only 4 individual non Kondo spins S: Their Curie constant equals $\alpha \times 4 \times S(S+1)$ while that of two pairs of spins, one F-like (spin $2S$), the other AF-like (spin 0), equals $\alpha \times 2S(2S+1) = \alpha \times 4 \times S(S+1/2)$. Hence the Curie constant is almost the same for large S values, whether the spins are RKKY-correlated in pairs at low temperature or uncorrelated at large temperature. A straightforward calculation provides a similar result in case of triplets, quadruplets ... when the ferromagnetic and antiferromagnetic RKKY couplings are of equal probability. In our case, if we assume $T_{K2} = 0$, we can write $\chi_{K2} = \alpha \times x_2 \times Sq/T$ with q varying from $S + 1/2$ to $S + 1$ when increasing the temperature. In contrast, the present pair hypothesis modify the magnetization analysis. Indeed, when the moments of each pair are correlated, only F-pairs (spin $2S$, concentration $x_2/4$) contribute to the magnetization: The latter equals $Ng\mu_B \times (x_2/4) \times 2S \times P_2$, i.e. half the second term of M in Eq.4. This implies a modification of formula Eq.5 as follows: $Y = P_1 + X \times P_2/2q$. Hence it is the saturated value of $P_2/2q$, instead of that of P_2/q, which has to be identified with the value 0.2 in Sec. IV B 2. It follows $q = 2.5$ since P_2 is a normalized polarization in the model, thus of saturated value equal to 1. Thus, we obtain three converging results when comparing the model and the data and assuming T_{K2} to equal strictly zero: $S = 2$ from the Brillouin fit of P_2, $q = (S + 1/2)$ to $(S + 1)$ from the susceptibility and $q = 2.5$ from the saturated value of the magnetization. So, at least for low moment concentrations, the present microscopic model appears to well account for the RKKY dominated term of the magnetization provided that one assumes $T_{K2} = 0$, an effective Mn spin equal to 2 and an equal number of the ferromagnetic and antiferromagnetic pairs.

The present model also allows to readily express the concentrations x_1 and x_2 in terms of π_0 the probability for a spin to be 'isolated' as previously done in Refs 1 and 28. In case of a perfect random distribution of the moments in space, $1 - x$ is the probability for any given atomic site to carry no spin. Hence $x_1 = x \times \pi_0$ and $x_2 = x \times (1 - \pi_0)$ where $\pi_0 = (1 - x)^Z$ with Z the number of atomic sites in a sphere with radius R_C: $Z = (4\pi/3) \times (R_C/a)^3$. For vanishing x ($x \ll 1/Z$), $x_1 \lesssim x$ and $x_2 \approx Z \times x^2$ (thus $\approx Z \times x_1^2$). The above (non simplified) $x_1(x, Z)$ and $x_2(x, Z)$ laws does not allow to fit, even poorly, our data over the whole $x = x_1 + x_2$ range. Here we calculate x_2 using $x_2 = x_2^*/q$ and $q = 2.5$ from the previous discussion. However the fits can be forced for samples as or less magnetic than $C - a$ ($x = 6 \times 10^{-4}$): See Fig.17, providing a value for Z: ≈ 530. (Note that we find actually $x_2 \propto x_1^{1.8}$ and that over our whole concentration range, see Sec. IV B.) Strikingly, this Z value yields a R_C value ($\approx 5 \times a$), thus obtained only for weakly magnetic samples, in excellent agreement with that ($5.3 \times a$) obtained from the above arguments
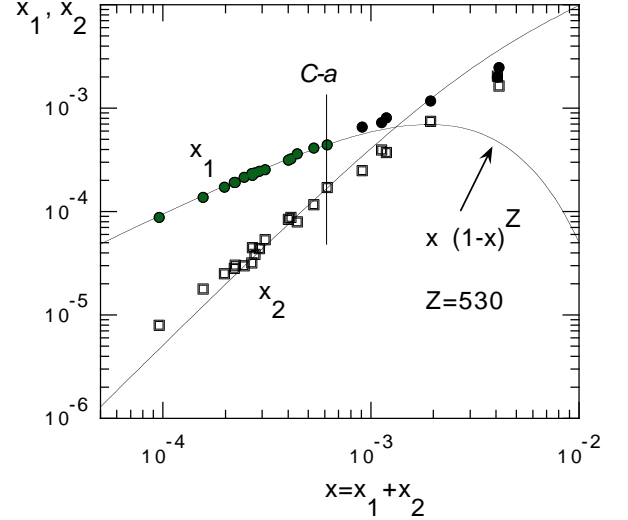

FIG. 17: x_1 (solid circles) and $x_2 = x_2^*/q$ (open squares) are plotted vs. $x_1 + x_2$ in a Log-Log diagram. Here, $q = 2.5$. The solid curve are the fitting curves with a simple $x_i(x, Z)$ dependence (See text), which roughly works only for samples less magnetic than sample $C - a$.

on the disappearance of the Kondo $\chi(1/T)$ curvatures in the more magnetic samples.

Up to now, we did not find any difference between the predictions of the Kondo cloud overlap and local competition RKKY$\times$ Kondo pictures, especially for low moment concentrations. However, the latter model could better explain the following two features exhibited by the more magnetic samples. First, for a sample of mean distance $\bar{r}$ between moments comparing with R_C, most $T_{J.loc}(i)$ compare with T_{K1}. Now the value of T_g reflects that of the $T_{J.loc}(i)$ averaged over all spins when no spin is Kondo-like. It follows that the T_g for a sample of $\bar{r} \sim R_C$ should compare with T_{K1} in the present assumption. It is exactly what we found experimentally for sample R where we associated $\bar{r}$ with R_C: Its T_g (3.6 K) compares with T_{K1} (3.35 K). The second feature is the discrepancy found between the experimental x_1 and x_2 and the $x_1(x, Z)$ and $x_2(x, Z)$ calculated for a perfect random distribution of Mn spins in the space. This discrepancy is all the more marked when the moment concentration increases: See the data and the $x_1(x, Z)$ and $x_2(x, Z)$ fitting curves extrapolated from the low moment concentration regime in Fig.17. A local RKKY $\times$ Kondo competition assumption allows to reconcile the data with the predictions made in case of a purely random spatial distribution of the moments. Indeed, a spin S_j separated from spin S_i by a distance smaller than R_C can generate a RKKY effect at site i partially cancelled by other spins lying more or less far away from site i. In consequence, a spin S_i at the center of a sphere of Z sites ($Z \propto R_C^3$) can be 'isolated' although other spins may lie inside the sphere. It follows that x_1 could be larger than $x \times (1 - x)^Z$ at large concentration. In conclusion, micro-

scopic models, especially that of a local RKKY$\times$ Kondo competition, account quantitatively for our results, including many details, over the whole here-studied $[T, H]$ range.

Let us end the present discussion by comparing our method of analysis and our results with previously published works where thermodynamic quantities (susceptibility, specific heat) were decomposed into two contributions. First, let us quote the magnetization analysis performed for dilute alloys, first for Fe in Cu in the early 70's[1]. The authors built a microscopic model of 'isolated' Kondo impurities and (almost non Kondo) impurity pairs to account for their results. In this case, because of the solubility limit of Fe in Cu, the largest studied moment concentration was small, equal to that of our sample $C - a$ (6×10^{-4}). Interesting enough, our results are similar to those for Fe in Cu in the same x-range ($< 6 \times 10^{-4}$). But, in addition, we could observe sizable low temperature $P_1(H)$ curvatures up to 70 kOe, which was not possible for Fe in Cu due to its large T_{K1} value (~ 12 K deduced following our procedure). For Fe in Cu, one could argue that the magnetization decomposition was actually forced by a chemical segregation of the Fe atoms into pair, triplets ... . But more essentially, the smallness of the Fe concentration, and thus of the averaged RKKY couplings, made these samples mainly Kondo dominated. Then one could argue the RKKY effect to give only a perturbative correction which simply adds to the Kondo susceptibility. Our results bring the question up again since, actually, the same magnetization decomposition holds up to concentrations where the RKKY couplings become dominant and thus cannot be anymore considered as a perturbation. Another example in the literature is the analysis of the magnetic specific heat C_P in Ce alloys[29]. It is the case for instance of $Ce(In_{3-y}Sn_y)$ where the moment concentration (which is large) is kept constant but where the random Sn substitution to In atoms induces environment fluctuations around each Ce atom. This makes the analysis much more complicated than in our case because the characteristics of each contributions (Kondo, RKKY) and not only their relative weight depend on the composition parameter y.

VI. CONCLUSION

We studied a system (QC $Al-Pd-Mn$) which belongs to the same category as the dilute alloys concerning the problem of the RKKY$\times$Kondo competition. However, it is a case where the few Mn atoms which carry an effective spin can be of broadly varying concentration whereas the Mn atoms are a component of the structure, of nearly fixed concentration. Because of the magnitude of the involved characteristic energy scales and the possibility to tune the moment concentration up to a point where the Kondo features disappear completely, we could obtain relevant results that we analyzed with no preconceived

assumptions. Surprisingly, we were led straightforwardly to a very simple result: The magnetization (and thus the susceptibility) is the sum of two contributions, one purely Kondo ($T_{K1} = 3.35$ K), the other one dominated by RKKY couplings. These two contributions coexist with the same characteristic temperatures, whatever the moment concentration up to that one where the RKKY interactions dominate fully. When building microscopical pictures, we found that different mechanisms (Kondo cloud overlap, RKKY) for breaking locally the Kondo effect account quantitatively for our data with an equal success. It is only by an analysis of the more magnetic samples, where the Kondo effects become negligible, that we could propose the local RKKY$\times$ Kondo competition as the best candidate to explain the local T_K depression. To conclude, we can ask the question whether all these models really correspond to a physics relevant at a microscopic level or provide a predictive picture for actually a more macroscopic and subtle physics such as two-fluids models do.

APPENDIX A: SINGLE-IMPURITY KONDO RESULTS

Only one energy scale, the Kondo temperature T_K, accounts for the single impurity magnetic behavior in the pure spin case (orbital moment $L = 0$). Hence a Kondo susceptibility $\chi_K(S, T, T_K)$ depending only on T, T_K and the spin value S. The Bethe *ansatz* calculations performed in the frame of the ($n = 2S$)-model showed that the temperature dependence of the susceptibility is the same for a spin $1/2$ and a spin larger than $1/2$[11,12]. So we first recall the results for a spin $1/2$. In the following, formula are written for a collection of spins, with concentration x, and N denotes the total number of atoms. Wilson[13] showed that the susceptibility χ_K can be expressed in terms of an implicit equation of the form: $\phi(y) = \ln(t)$ where $\phi(y)$ is a universal function of y. Here, $t = T/T_K$, y is the relative deviation of the Kondo susceptibility χ_K from the Curie law C/T: $y = (\chi_K - C/T)/(C/T)$ and the Curie constant C is calculated for a spin $1/2$: $C = \alpha x(3/4)$ with $\alpha = N(g\mu_B)^2/3k_B$. To evaluate $\chi_K(T, T_K)$ amounts to calculate $y(t)$. One can write $\chi_K(T, T_K) = (C/T_K)(y(t)+1)/t$ and thus $\chi_K(T) = \chi_K(T = 0)F(t)$ where $\chi_K(T = 0) = Cw/T_K$ and, by definition, $F(t = 0) = 1$. The value of the parameter w depends on the definition of T_K. That given by Wilson from a precisely defined procedure extended to very high T[13] yields $w = \pi^{-3/2} \times e^{(c+1/4)} = 0.4107\ldots$ (c is the Euler's constant)[2]. In summary:

$$\chi_K(S = 1/2, T, T_K) = \frac{0.308\alpha x}{T_K} F(\frac{T}{T_K}), \qquad (A1)$$

We used the following results in order to build the function $F(T/T_K)$. For $T/T_K > 30$, y remains of moderate value and perturbation theory can be applied. Hence

we can deduce χ_K (to better than 1%) from an asymptotic analytic formula for $\phi(y)$. Following Wilson[13]: $\phi(y) = -1/y - 0.5\ln|y| + 1.5824y$. For lower t values, the behavior is fundamentally non-perturbative. Thus, for $t = 0.1$ to 28, we used the renormalization results in Ref.14. Close to $T = 0$, the Fermi liquid approach[30] provides: $\chi_K(T)/\chi_K(T=0) = 1 - at^2$ where $a = \sqrt{3}\pi^3 w^2/8$ (half the value of the a in Ref.2 due to a typing error in the quoted book). Note that one can approximate the Kondo susceptibility by a Curie-like term at large temperatures. It is because, the $\chi_K(T)$ is dominated by the C/T term and the corrections, because they are logarithmic, can be averaged over a restricted T-range. For instance, $F(t)/T_K$ in formula Eq.A1 nearly equals $1.65/T$ for $20 < t < 1.5 \times 10^3$, hence: $\chi_K = C'/T$, with $C' = 1.65 \times Cw \approx 0.68 \times C$, to better than 2%.

To treat the case $S > 1/2$, one can use the n-channel Kondo model with $n = 2S$ which yields a completely spin-compensated ground state. In the frame of this model, Bethe *ansatz* calculations which previously were shown to treat successfully the $(S = 1/2)$-case[31] have been carried out for $S > 1/2$. The results are the following[11]. For $n = 2S$, the susceptibility reaches a saturated value $\chi_n(T=0)$ at $T = 0$. When one defines the Kondo temperature T'_K as given from formula[2,11,12]: $\chi_n(T=0) \propto n/\pi T'_K$ (hence $\propto S/\pi T'_K$ and not $\propto S(S+1)/T'_K$), $\chi_n(T)/\chi_n(T=0)$ is found to be an almost n-independent function of T/T'_K at low and moderate T/T'_K. Hence the $(n = 2S)$-expression :

$$\chi_K(S,T,T'_K) = \frac{3\alpha x S}{\pi T'_K}\psi(\frac{T}{T'_K}) \ \text{ with } \ \psi(0) = 1 \qquad (A2)$$

where $\psi(T/T'_K)$ is S independent. Other authors checked the validity of this model by comparing their theoretical results to experimental susceptibility, resistivity and specific heat data obtained for some dilute alloys[12,32]. Formula Eq.A2 is equivalent to: $\chi_K(S,T,T'_K) = n \times \chi_K(S = 1/2,T,T'_K)$. So, the present definition of T'_K makes the low temperature susceptibility of a spin $S = n/2$ to behave as that of n independent spins 1/2 having the same T'_K value. When identifying the $\chi_n(T=0)$ in Formula Eq.A2 for $S = 1/2$ with the $\chi_K(T=0)$ of Wilson, one finds the relation between the values of T'_K and the Wilson's T_K: $T'_K = 2T_K/(\pi w)$, which allows to rescale formula Eq.A2 using the Wilson's T_K:

$$\chi_K(S,T,T_K) = n \times \chi_K(S = 1/2,T,T_K), \ n = 2S \quad (A3)$$

where $\chi_K(S = 1/2)$ is given in Eq. A1, For $T > T'_K$, deviations of $\psi(T/T'_K)$ with the $S = 1/2$ results occur, increasing with $\text{Log}(T/T'_K)$. These deviations are unnoticeable in the $\chi_n(T)/\chi_n(0)$ curves shown in Fig.1 in Ref.11. But they can be calculated from the $T\chi_n(T)/B_n$ curves in the same diagram. B_n denotes the standard Curie constant: $B_n \propto S(S+1)$. These deviations are expected since Eq.A3 gives an odd limit for $\chi_K(S,T,T_K)$, $S > 1/2$, when $T/T'_K \to \infty$. Indeed, the expected limit is

the susceptibility of non Kondo spins: $\chi = \alpha x S(S+1)/T$ whereas that one calculated from Eq.A3 equals n times the limit for $S = 1/2$ and thus $\alpha x S(3/2)/T$. From the $T\chi_n(T)/B_n$ curves in Fig.1, Ref.11, one finds a good approximation to account for the present deviations for $1 < T/T'_K < 20$: $\psi(S = 5/2, T/T'_K) \approx \psi(S = 1/2, T/T'_K) \times (1 + \epsilon)$ where $\epsilon = 0.0035 \times (T/T'_K)$. In our case, we found $T_{K1} = 3.35$ K (T'_K =5.2 K) from the two-T_K analysis carried out for $2 \text{ K} \leq T \leq 100$ K ($0.4 < T/T'_K < 19$) neglecting these deviations. When using the $(1 + \epsilon)$-correction, we find a T_{K1} only about 10% smaller than the previous estimate. We conclude that our analysis above 2 K gives correct results. For T/T'_K much larger than 20, the deviations of $\psi(T/T'_K)$ from the $S = 1/2$ results are larger. We do not want to make any assumption, except that χ_K should equal $\alpha x S(S+1)/T$ with logarithmic corrections[33,34]. This is the reason for which we write $\chi_K = \alpha \times Sq/T$, $q < S+1$, over restricted high-T ranges ($q = S+1$ is achieved for T_K strictly equal to zero in case of finite T). Finally, let us give the reason why we chose the $n = 2S$ results instead of a Curie-Weiss (C.W.) law: $\chi_K = A/(T+\theta)$ to fit our data. The C.W. fits provide unreliable estimates of T_K since θ/T_K depends on the t range: For instance, one finds $\theta = 1.34 \times T_K$ for $1 < t < 20$, $\theta = 2.77 \times T_K$ for $10 < t < 100$, $\theta = 3.32 \times T_K$ for $20 < t < 1500$ from the fit of the function $F(t)$ with a (C.W.) law. Therefore, from the θ value found for temperatures covering one or two decades of t, it is impossible to predict accurately the susceptibility for much lower (or larger) temperatures.

APPENDIX B: P(T_K) DISTRIBUTION EFFECT

In many experimental works devoted to Kondo alloys, the susceptibility has been analyzed with the minimum number of values of T_K (or θ from C.W. laws), necessary to account for the data. For instance, in the case of dilute alloys such as Cu-Fe[1], Pt-Co[28], two θ values were necessary for an analysis carried out down to low temperatures. Of course, it is the only possible method for analyzing the data in a simple way. However, such an analysis can hide the existence of a distribution of T_K as we discuss now. Let us take an over-simplified example, that of a flat normalized distribution: P(T_K) $= 1/(T_{Kmax} - T_{Kmin})$ for $T_{Kmin} \leq T_K \leq T_{Kmax}$ and P(T_K) $= 0$ elsewhere. The calculation of the average susceptibility $\overline{\chi(T)} = \int \chi(T,T_K) \times P(T_K)dT_K$ is very simple when one uses a Curie-Weiss-like laws for $\chi(T,T_K)$: This yields qualitatively the results given in the following. However, we used the Wilson's law A1, namely: $\chi \propto (x/T_K) \times F(T/T_K)$, to calculate numerically $\overline{\chi}$ in the two following cases. The first case is that of a T_K distribution rather narrow in view of the $\ln(T)$ susceptibility feature. Taking $T_{Kmin} = T_{Kmax}/3$, one finds a $\overline{\chi}$ obeying a single-T_K law: $\overline{\chi} = (x^*/T_K^*) \times F(T/T_K^*)$ over a wide T/T_K^* range, from 10^{-2} to 10^2. The value of x^* is found to be almost equal to that of x: $x^* = 0.96 \times x$ and
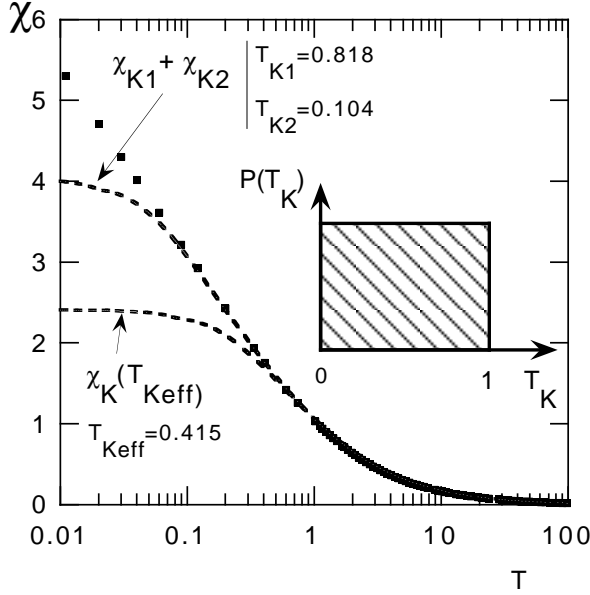
FIG. 18: The solid squares represent the $\overline{\chi(T)} = \int \chi(T, T_K) \times P(T_K) dT_K$ calculated for the $P(T_K)$ shown in the figure. Here the temperatures are in T_{Kmax} units. The fits with a single-T_K and a two-T_K model for $1 < T < 100$ are extrapolated down to $T = 0.01$, which shows the domain of validity for the approximation of $\overline{\chi(T)}$ as a sum of a limited Kondo terms

$T_K^* \approx T_{Kmax}/\sqrt{3}$. This result shows that a narrow distribution of T_K is undetectable from the analysis of measured susceptibility. The second case is that of a broad distribution $P(T_K)$ spreading down to $T_{Kmin} = 0$. See Fig.18: $\overline{\chi}$ can be accurately fitted over two temperature decades, from $T/T_{Kmax} = 1$ to 100, by a single-T_K Kondo susceptibility with $T_K^* = 0.415 \times T_{Kmax}$. Here again, x^* almost equals x: $x^* = 0.99 \times x$. In the same T/T_{Kmax} range, $\overline{\chi}$ can be also fitted by a two-T_K model, which yields: $x_1 = 0.63 \times x$, $T_{K1} = 0.818 \times T_{Kmax}$, $x_2 = 0.42 \times x$ and $T_{K2} = 0.104 \times T_{Kmax}$. When the T/T_{Kmax}-range is extended to a third temperature decade, namely down to 0.05, the $\overline{\chi}$ behavior cannot be described by a single-T_K model anymore, but can be accounted for by two-T_K model with parameters values (x_i and T_{Ki}) close to those found at $T/T_{Kmax} > 1$. In summary one has: $T_{K2} < T_K^* < T_{K1}$ and $x_1 + x_2$ close to the x^* value found from a single-T_K fit performed over the two previous temperature decades. Thus, we conclude that, when a sum of two Kondo susceptibilities is necessary to account for experimental data over a wide temperature range, one may actually deal with a distribution of T_K, spreading over a large T_K range.

* Corresponding author: jean-jacques.prejean@grenoble.cnrs.fr
[1] J.L. Tholence and R. Tournier, Phys. Rev. Lett. **25**, 867 (1970)
[2] A.C. Hewson, *Cambridge Studies in Magnetism*, edited by D. Edwards and D. Melville (Cambridge University Press, 1993).
[3] P. Nozières and A. Blandin, J. Phys. (Paris) **41**, 193 (1980)
[4] J.C. Lasjaunias, A. Sulpice, N. Keller, J.J. Préjean and M. de Boissieu, Phys. Rev. B **52**, 886 (1995)
[5] F. Hippert, M. Audier, J.J. Préjean, A. Sulpice, E. Lhotel, V. Simonet and Y. Calvayrac, Phys. Rev. B **68**, 134402 (2003).
[6] K. Binder, Solid State Comm. **42**, 377 (1982).
[7] J.J. Préjean, C. Berger, A. Sulpice and Y. Calvayrac, Phys. Rev. B **65**, 140203 (2002).
[8] C. Berger and J.J. Préjean, Phys. Rev. Lett. **64**, 1769 (1990).
[9] J. Dolinšek, M. Klanjšek, T. Apih, J. L. Gavilano, K. Giannò, R. H. Ott, J. M. Dubois and K. Urban, Phys. Rev. B **64**, 24203 (2001).
[10] V. Simonet, F. Hippert, C. Berger and Y. Calvayrac, in *Proceedings of the 8th International Conference on Quasicrystals, Bangalore, 2002*, J. Non-Cryst Solids **334-335**, 408 (2004).
[11] H.U. Desgranges, J. Phys. C **18**, 5481 (1985)
[12] P. Schlottmann and P. D. Sacramento, Adv. in Phys., **42**, 641 (1993) and References therein.
[13] K.G. Wilson, Rev. Mod. Phys. **47**, 773 (1975)
[14] H.R. Krishna-murthy, J.W. Wilkins and K.G. Wilson, Phys. Rev. B **21**, 1003 (1980).
[15] P. Nozières, Eur. Phys. J B **6**, 447 (1998).
[16] M.A. Chernikov, A.Bernasconi, C. Beeli, A. Schilling and H.R. Ott, Phys. Rev. B **48**, 3058 (1993).
[17] C.A. Swenson, I.R. Fisher, N.E. Anderson, Jr., P.C. Canfield and A. Migliori, Phys. Rev. B **65**, 184206 (2002).
[18] P.D. Sacramento and P. Schlottmann, J. Phys.: Condens. Matter **3**, 9687 (1991).
[19] In the quoted Figure (where the scaling variable has to be corrected by replacing H/T_H by H/T_1), the author represents the variation of $M(T = 0, S = 1/2)$ with $g\mu_B H/k_B T_1$. The T_1 is defined as follows: $T_1 = (8/\pi e)^{1/2} \times T_K/w$, that we calculated for T_K=3.35 K to plot the solid curve in Fig.16.
[20] C.L. Lin, A. Wallash, J.E. Crow, T. Mihalisin and P. Schlottmann, Phys. Rev. Lett. **58**, 1232 (1995)
[21] V. Barzykin and I. Affleck, Phys. Rev. B **61**, 6170 (2000).
[22] V. Dobrosavljevic, T.R. Kirkpatrick and G. Kotliar, Phys. Rev. Lett. **69**, 1113 (1992)
[23] S. Roche and D. Mayou, Phys. Rev. B **60**, 322 (1999).
[24] D. Mayou, Phys. Rev. Lett. **85**, 1290 (2000).
[25] P. Schlottmann, Phys. Rev. Lett. **80**, 4975 (1998).
[26] M. Garst, S.Kehrein, T.Pruschke, A. Rosch and M. Vojta, Phys. Rev. B **69**, 214413 (2004)
[27] P. Nozières in *Kondo effect - 40 years after the discovery* [J. Phys. Soc. Jpn **74**, 4 (2005)]
[28] B. Tissier and R. Tournier, Solid State Comm. **11**, 895 (1972)
[29] A.M. Lobos, A.A. Aliglia and J.G. Sereni, Eur. Phys. J B **41**, 289 (2004).
[30] P. Nozières, J. Low Temp. Phys. **17**, 31 (1974) and

Low Temperature Physics Conference Proceedings LT14 **5**, edited by M. Krusius and M. Vioro , (Elsevier, New York, 1975).

[31] N. Andrei, K. Furuya and J.H. Lowenstein, Rev. Mod. Phys. **55**, 331 (1983)

[32] P. Schlottmann, Physics Reports **181**, 1 (1989)

[33] N. Andrei and C. Destri, Phys. Rev. Lett. **52**, 364 (1984)

[34] P. Schlottmann and P.D. Sacramento, Physica B **206 - 207** 95 (1995)